Confinement-induced valence-band mixing in CdS quantum dots observed by two-photon spectroscopy

K. I. Kang,* B. P. McGinnis, Sandalphon, Y. Z. Hu,* S. W. Koch,* and N. Peyghambarian
Optical Sciences Center, University of Arizona, Tucson, Arizona 85721

A. Mysyrowicz
Ecole Polytechnique–Ecole Nationale Supérieure de Techniques Avancées, Laboratoire d'Optique Appliquée, Palaiseau, France

L. C. Liu and S. H. Risbud
Department of Mechanical, Aeronautical, and Materials Engineering, University of California, Davis, California 95616
(Received 3 June 1991, revised manuscript received 28 October 1991)

One- and two-photon absorption spectra of the quantum-confined transitions of CdS quantum dots are reported. The results show significant deviations from calculations based on the parabolic-valence-band approximation. The near-degenerate one- and two-photon transitions observed experimentally, and confirmed theoretically using Luttinger theory and numerical matrix diagonalization, clearly demonstrate the effects of valence-band mixing and Coulomb interaction.

The confinement of electron-hole pairs in semiconductor microcrystallites can result in discrete optical transitions if all three dimensions are sufficiently small. From a fundamental point of view these microcrystallites, often called quantum dots, represent an intriguing system comprising both the discrete nature of isolated elements and the band nature of large-ordered systems. At present, quantum dots are still insufficiently understood due to the complexity of the system with a large uncharacterized distribution of sizes, shapes, stoichiometry, defects, and surface interactions. Most of the information so far has been obtained from optical methods of investigation such as one-photon absorption,[1] photoluminescence,[2,3] four-wave mixing,[4] laser pump and probe techniques,[5,6] nonlinear bleaching,[7] far-infrared magnetospectroscopy,[8] and dc-electric-field-induced transmission changes.[9–11] Most quantum dots to date exhibit broad absorption resonances that become sharper with decreasing dot radius. These resonances are usually assigned to quantum-confined states based on a simple model which assumes simple parabolic valence and conduction bands. This model has been successful in describing the optical nonlinearities of quantum dots measured in pump-probe experiments.[6] However, recent theoretical publications[12,13] indicate that this model needs to be modified to account for mixing of the valence bands caused by the spherical confining potential of small quantum dots. In this paper, we present experimental verification of such confinement-induced valence-band mixing by measuring and comparing one- and two-photon absorption spectra of CdS quantum dots in glass. Because of the large number of poorly known system parameters, one-photon absorption measurements alone are not sufficient to determine unambiguously the energies between the quantum-confined states. However, the combination of one- and two-photon absorption spectra allow a direct comparison of electron-hole pair states with total angular momentum 0 and 1, thus eliminating much of the experimental uncertainties. We find that our experimental results can only be explained by a model that takes into account valence-band mixing.

In the simple model most commonly used to describe semiconductor quantum dots, a spherical infinite potential of radius R surrounds a semiconductor material described by a single parabolic conduction band and a single parabolic valence band. Neglecting Coulomb interactions, the electron-hole-pair envelope wave functions are separable and are products of spherical Bessel functions and spherical harmonics. The two lowest energetic states for the electrons and holes are diagramed in Fig. 1(a). The labels s and p correspond to the angular momentum states $l=0$ and 1, while the subscripts e and h correspond to the electrons and holes. In this simple model, one-photon transitions are allowed for $\Delta l=0$, while two-photon transitions are allowed for $\Delta l=\pm 1$. Inclusion of the Coulomb interaction between the electron and hole perturbs the electron and hole wave functions, but each band state maintains its dominant character, allowing us to retain the same labels for each state.[14] Within this simple model, one can calculate the one- and two-photon absorption spectra for CdS quantum dots, as shown in Fig. 1(b). Effective masses appropriate for the A band in bulk wurtzite CdS, $m_e \simeq 0.2m_0$ and $m_h \simeq 1.35m_0$ [$m_\perp = 0.7m_0$, $m_\parallel = 5m_0$, and thus $m_h = \sqrt[3]{(m_\perp^2 m_\parallel)} = 1.35m_0$] have been used. A phenomenological broadening parameter has been introduced to account for the homogeneous linewidth and the inhomogeneous contribution from the distribution of dot sizes. The energy differences between the peaks observed in one- and two-photon absorption (as schematically shown by vertical lines) are due to the different allowed transitions, as can

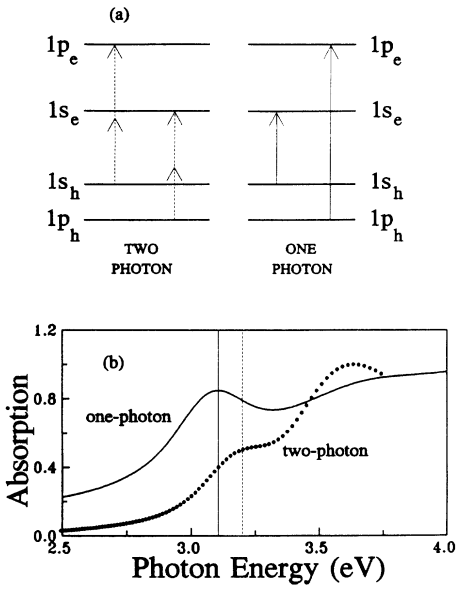

FIG. 1. (a) One- and two-photon-allowed transitions between the discrete states in the spherical potential well; (b) theoretical calculation of one- and two-photon absorption based on a parabolic band model.

be verified by examining Fig. 1(a). These energy differences are related to the ratio of electron and hole effective masses by

$$\frac{E_{(1p_h-1s_e)}-E_{(1s_h-1s_e)}}{E_{(1s_h-1p_e)}-E_{(1s_h-1s_e)}}=\frac{E_{(1p_h-1p_e)}-E_{(1s_h-1p_e)}}{E_{(1p_h-1p_e)}-E_{(1p_h-1s_e)}}=\frac{m_e}{m_h}\,, \tag{1}$$

where E is the energy of the subscripted transition. Using the masses for CdS, the first two-photon resonances are expected to be situated between the first two one-photon transitions, as seen in Fig. 1(b). The splitting between the one- and two-photon absorption peaks is a result of the nondegeneracy of the valence-band states. By experimentally measuring both the one- and two-photon absorption spectra, we can check the predictions of this model, which assumes a single uncoupled parabolic valence band for these quantum dots.

For our experiments, we used samples containing CdS microcrystallites in a glass matrix. The samples were synthesized by first melting and casting an oxide glass melt of nominal batch composition: 56% SiO_2, 24% K_2O, 9% BaO, 8% B_2O_3, and 3% CaO (in weight % of each oxide). Powders were ground from this glass, mixed with 0.5–1 wt % CdS, and the batch was remelted in alumina crucibles at 1400 °C for 1.5 h. Glass samples containing dissolved CdS in solution were obtained and sections cut from the same slab were reheated to induce the growth of variously sized quantum dots. The samples containing CdS quantum dots have been analyzed[15] to obtain their size distribution by field-effect scanning electron microscopy and differential thermal-analysis techniques. It is well documented that the average radii of the quantum dots increase with higher temperatures and longer treatment times. Heat-treated samples were cut and polished to dimensions of approximately $1\times3\times10$ mm^3. The samples were mounted onto a cold finger inside a closed-cycle helium cryostat that cooled the samples to approximately 10 K. The sample with the smallest microcrystallites had average radii of 0.9 ± 0.7 nm, while the sample with the largest microcrystallites had average radii of 8.0 ± 0.7 nm; confinement effects are considered important for microcrystallite radii comparable to or smaller than the bulk exciton Bohr radius, which is 3 nm for CdS. The distribution of dot sizes in each sample increases the bandwidth of the absorption resonances and limits the resolution of the spectroscopic measurements.

Optical characterizations consisted of both one- and two-photon absorption measurements for each sample. One-photon spectra were obtained through direct transmission measurements or by excitation spectroscopy. Two-photon spectra were obtained through two-photon excitation spectroscopy where the photoluminescence (PL) intensity is detected as the excitation frequency is varied at constant input-intensity excitation. Most of the PL from our samples was emitted in a broad band, peaking near 800 nm. These PL spectra were observed to be independent of the excitation photon energy, allowing us to monitor a constant band of PL while tuning the ex-

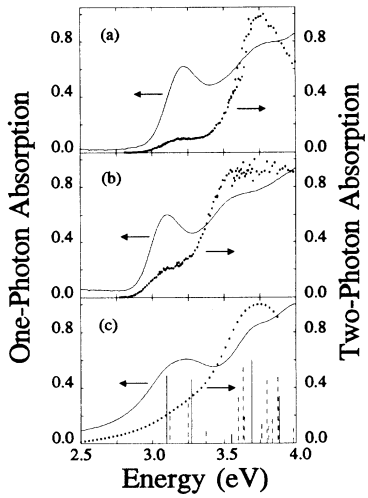

FIG. 2. (a) Experimental results of one-photon (solid line) and two-photon (dots) absorption spectra for a quantum-dot sample heat treated at 640 °C for 1 h. No observable differences are seen in the transition energies between the one- and two-photon spectra. (b) Similar experimental results for a quantum dot sample heat treated at 640 °C for 3 h. (c) Calculations of one-photon (solid line) and two-photon (dots) absorption spectra based on the Luttinger Hamiltonian. The vertical lines are calculated with no broadening, while the dashed and solid curves represent spectra for a broadening of $\gamma=8E_R$, where E_R is the bulk exciton binding energy of 27 meV. The magnitude of a vertical line represents the absorption strength. The other parameters used in the calculations are $R/a_B=0.5$, with $\gamma_1=2.97$ and $\mu=0.75$. The experimental data of (a) and (b) should be compared with (c).

citation source to obtain the two-photon absorption spectrum. The validity of this technique was checked by obtaining one-photon absorption spectra through PL excitation, comparing it to absorption spectra obtained from transmission measurements, and verifying that the two techniques give identical results.

PL was collected at right angles to the excitation beam and evaluated only for wavelengths shorter than the excitation lasers in order to ensure that no scattered light or one-photon-induced PL corrupted the measurement. We verified that the collected PL follows the expected quadratic dependence on pump energy for the two-photon spectra. The excitation sources for two-photon spectra were a Ti:sapphire laser and an amplified DCM dye laser pumped with an injection-seeded pulsed Nd:YAG (yttrium aluminum garnet) laser, which covered the combined spectral range 600–930 nm. The excitation beams were focused to a 0.5-mm-diameter waist, and excitation energies were maintained at 1 and 0.1 mJ for the Ti:sapphire and dye laser beams, respectively. Spectra were obtained with constant excitation pulse energies, discriminated to within 5% of the mean. The laser-pulse temporal profiles were digitized for every tuning and stored for later analysis of the two-photon absorption spectra.

Examples of the one- and two-photon spectra for two samples with different average quantum dot radii between 1 and 2 nm are shown in Figs. 2(a) and 2(b). It is apparent that the one- and two-photon absorption peaks occur at the same energies. Similar spectra were obtained for other quantum dot samples with different average sizes. The poor agreement between the experimental spectra in Figs. 2(a) and 2(b) and the theoretical spectra in Fig. 1(b) shows that the independent parabolic-valence-band approximation is insufficient to explain the optical transitions of CdS quantum dots.

To improve the model, we performed a theoretical analysis, which includes mixing of the heavy- and light-hole valence bands induced by the spherical confining potential.[12,13] The eigenstates of the electron-hole pairs in the quantum dot satisfy the Hamiltonian

$$H=-\frac{\hbar^2}{2m_e}\nabla_e^2+H_L-\frac{e^2}{\epsilon|\mathbf{r}_e-\mathbf{r}_h|}\ , \tag{2}$$

where H_L is the Luttinger Hamiltonian for the valence bands in a spherical coordinate system[16,17]

$$H_L=\frac{\gamma_1}{2m_0}\left[p^2-\frac{\mu}{9}(\mathbf{p}^{(2)}\times\mathbf{J}^{(2)})\right]\ , \tag{3}$$

with $\mathbf{p}$ denoting the hole linear momentum operator, $\mathbf{J}$ the angular momentum operator, and $\mathbf{p}^{(2)}$ and $\mathbf{J}^{(2)}$ the second-rank irreducible tensor operators of the momentum $\mathbf{p}$ and the angular momentum $J=\frac{3}{2}$, respectively. The coupling constant μ is

$$\mu=\frac{4\gamma_2+6\gamma_3}{5\gamma_1}\ , \tag{4}$$

with γ_1, γ_2, and γ_3 being the Luttinger parameters. Equation (3) is a simplified version of the Luttinger-Kohn Hamiltonian for the case of $(\gamma_3-\gamma_2)\ll\gamma_1$.[16] In the numerical calculation, we choose the eigenstates of the square of the total pair angular momentum and its z component as the basis into which the Hamiltonian is expanded and diagonalized. The Coulomb energy is included, as discussed in Refs. 6 and 14. The numerically computed one- and two-photon absorption spectra from this model using parameters appropriate for cubic CdS ($\mu=0.75$) are shown in Fig. 2(c). The vertical lines in this figure represent the energetic positions of the transitions and their oscillator strengths. There are several predicted new resonances that satisfy the selection rules of total angular momentum, including quantum confinement and Coulomb interaction. The solid and dashed curves show the one- and two-photon absorption spectra calculated with a broadening of $\gamma=8E_R$, where $E_R=27$ meV is the bulk exciton binding energy. We see that the resonances merge and form an absorption curve that agrees well with the experimental data.

The near degeneracy of the one- and two-photon transition energies observed here results from the fact that the two lowest energy-hole states are roughly degenerate for the case of CdS quantum dots. This can be easily seen in Fig. 3, where the calculated energy of the two lowest hole states, labeled $s_{3/2}$ and $p_{3/2}$ to indicate their s- and p-like characters, are plotted as a function of the coupling constant μ for a quantum dot radius equal to half of the bulk exciton radius. In the vicinity of $\mu=0.75$, which is appropriate for CdS, we see that the two curves nearly touch, suggesting near degeneracy caused by the confinement-induced modification of the original heavy- and light-hole states. Figure 3 indicates that for materials with smaller coupling constant μ values, these states are nondegenerate and the one- and two-photon transition energies are not expected to coincide. It is noted that the results of Fig. 3 are not strongly size dependent for the range of quantum dot sizes analyzed in this study. For very large dot sizes the assumptions made in the calculations are no longer valid, and the treatment does not

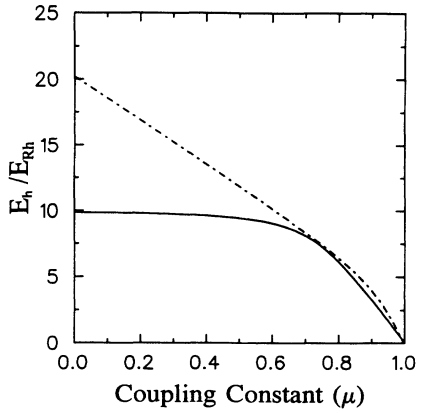

FIG. 3. Calculated normalized energies of the two lowest valence-band states, $s_{3/2}$ and $p_{3/2}$, in the quantum dot with crystallite size of $R=a_{hB}$. Here E_{Rh} and a_{hB} are the Rydberg energy and the Bohr radius computed for the hole. The solid line (dashed line) represents the $s_{3/2}$ ($p_{3/2}$) states.

apply.

In conclusion, spectroscopic analysis of one- and two-photon absorption spectra of CdS quantum dots indicates that the quantized states of the holes develop from a mixture of the bulk light- and heavy-hole valence bands. Previous models, which only describe uncoupled valence bands in the parabolic-band approximation, do not accurately describe our experimental spectra. A good fit to the experimental results is obtained when the mixing of the light- and heavy-hole valence bands due to the spherical confining potential is included in the Luttinger Hamiltonian calculations. Further improvements in the production of quantum dots should reveal the detailed spectrum of two-photon resonances predicted with this model.

The authors would like to acknowledge support from NSF (Grant Nos. ECS89-09913 and DMR90-06282), Joint Services Optical Program, ARO (Grant No. DAAL03-89-K-0100), SDI/ONR (Grant No. N00014-91-J-1619), NATO (Travel Grant No. 86-0749), and the Optical Circuitry Cooperative of the University of Arizona.

---

*Also at the Physics Department of the University of Arizona.

[1]A. I. Ekimov and A. A. Onushchenko, Pisma Zh. Eksp. Teor. Fiz. **40**, 337 (1984) [JETP Lett. **40**, 1136 (1984)].

[2]M. G. Bawendi, W. L. Wilson, L. Rothberg, P. J. Carroll, T. M. Jedju, M. L. Steigerwald, and L. E. Brus, Phys. Rev. Lett. **65**, 1623 (1990).

[3]H. Shinojima, J. Yumoto, N. Uesugi, S. Omi, and Y. Asahara, Appl. Phys. Lett. **55**, 1519 (1989).

[4]D. W. Hall and N. F. Borrelli, J. Opt. Soc. Am. B **5**, 1650 (1988).

[5]P. Roussignol, D. Richard, C. Flytzanis, and N. Neuroth, Phys. Rev. Lett. **62**, 312 (1989).

[6]Y. Z. Hu, S. W. Koch, M. Lindberg, N. Peyghambarian, E. L. Pollock, and F. F. Abraham, Phys. Rev. Lett. **64**, 1805 (1990).

[7]Y. Wang, N. Herron, W. Mahler, and A. Suna, J. Opt. Soc. Am. B **6**, 808 (1989).

[8]Ch. Sikorski and U. Merkt, Phys. Rev. Lett. **62**, 2164 (1989).

[9]F. Hache, D. Ricard, and C. Flytzanis, Appl. Phys. Lett. **55**, 1504 (1989).

[10]V. Esch, B. Fluegel, G. Khitrova, H. M. Gibbs, Xu Jiajin, K. Kang, S. W. Koch, L. C. Liu, S. H. Risbud, and N. Peyghambarian, Phys. Rev. B **42**, 7450 (1990).

[11]S. Nomura and T. Kobayashi, Solid State Commun. **73**, 425 (1990).

[12]J. B. Xia, Phys. Rev. B **40**, 8500 (1989).

[13]K. J. Vahala and P. C. Sercel, Phys. Rev. Lett. **65**, 239 (1990).

[14]Y. Z. Hu, M. Lindberg, and S. W. Koch, Phys. Rev. B **42**, 1713 (1990).

[15]L. C. Liu and S. H. Risbud, J. Appl. Phys. **68**, 28 (1990); Philos. Mag. Lett. **61**, 327 (1990).

[16]A. Balderschi and N. U. Lipari, Phys. Rev. B **8**, 2697 (1973).

[17]J. M. Luttinger, Phys. Rev. **102**, 1030 (1956).